Liquid Crystals
Publication details, including instructions for authors and subscription information:
http://www.informaworld.com/smpp/title~content=t713926090

Modelling of addressing schemes in surface stabilized ferroelectric liquid crystal cells using a three variable model in one dimension

S. M. Said; S. J. Elston

Online publication date: 11 November 2010

To cite this Article Said, S. M. and Elston, S. J.(2002) 'Modelling of addressing schemes in surface stabilized ferroelectric liquid crystal cells using a three variable model in one dimension', Liquid Crystals, 29: 2, 263 — 271
To link to this Article: DOI: 10.1080/02678290110096397
URL: http://dx.doi.org/10.1080/02678290110096397

LIQUID CRYSTALS, 2002, VOL. 29, NO. 2, 263–271

Modelling of addressing schemes in surface stabilized ferroelectric liquid crystal cells using a three variable model in one dimension

S. M. SAID* and S. J. ELSTON

Department of Engineering Science, University of Oxford, Parks Road, Oxford OX1 3PJ, UK

(*Received 16 February 2001; in final form 7 August 2001; accepted 16 August 2001*)

The 'Three-Variable Model in One Dimension' has been successfully used to model the domain switching process for simple monopolar and bipolar pulses. In this paper, we discuss the development of this model to describe the switching process due to more complicated addressing waveforms. We have taken two contrasting addressing schemes: the Seiko scheme which is a simple example of a low voltage addressing scheme, and the Joers Alvey scheme, a high voltage addressing scheme which utilizes the high biaxiality properties of a ferroelectric liquid crystal (FLC) material. We experimentally simulate the voltage sequence 'seen' by a pixel subject to these addressing schemes, and take into consideration the worst case combinations of voltages that could cause switching and non-switching conditions. We show that the 'Three Variable Model in One Dimension' is in excellent agreement with experimental data for the Seiko addressing scheme, and can be used to predict the operating regime for the Joers Alvey addressing scheme.

1. Introduction

A typical surface stabilized ferroelectric liquid crystal (SSFLC) display consists of horizontal (rows) and vertical (columns) stripe electrodes, where the area of overlap between a row and a column forms a pixel. Each pixel is subject to a superposition of voltage sequences delivered to its electrodes, and switching occurs when a pulse of critical time–voltage (t–V) product is applied. Many multiplexing schemes [1–4] have been devised to address the pixels within such displays, their aim being to obtain as short a selection time as possible and to deliver good optical contrast.

2. Types of addressing schemes

For an array of pixels, an image may be created by sequentially (row by row) applying a selection waveform to a row whilst supplying data waveforms simultaneously to all columns. Typically, the data waveforms are assigned values of $\pm V_D$ and the selection waveforms are assigned values of $\pm V_S$, where $V_D < V_D$. In the cases that we shall discuss, the selection waveform is only applied during the control window of addressing, of time width T_a, the line addressing time. Therefore, the selection and data waveforms only superimpose during the control window, resulting in switching of the ferroelectric polarization either up or down, leading, respectively, to a dark or bright optical state for the display.

We refer to figure 1, which is a typical time–voltage (t–V) plot for switching due to a bipolar pulse, for an SSFLC cell with high biaxiality. We can use this plot as a basis for two principal ideas in developing an addressing scheme: the low voltage scheme (represented by the solid line), and the high voltage scheme (represented by the dotted line). In the low voltage scheme, a pixel with the applied voltage amplitude of $(V_{SL} + V_D)$ will switch to the opposite state whilst $(V_{SL} - V_D)$ will leave the pixel in its original state. The pixels in the non-addressed rows see $\pm V_D$ which is too small to switch them. The high voltage scheme exploits the t–V_{min} property of a material with high biaxiality. The principle in operation is the opposite of the principle for the low voltage scheme, i.e. $(V_{SH} + V_D)$ is the non-switching voltage, whilst $(V_{SH} - V_D)$ is the switching voltage. The high voltage addressing scheme has the advantage of being able to employ a faster switching time, albeit at the expense of having to use a higher operating voltage.

2.1. *The Seiko scheme*

The Seiko scheme, as shown in figure 2, is the simplest example of a low voltage scheme. If the data and selection waveforms are of the same polarity within the control window, the pixel experiences a smaller voltage $(V_S - V_D)$ that is not supposed to affect the pixel's state.

*Author for correspondence;
e-mail: suhana.mohd-said@eng.ox.ac.uk

Liquid Crystals ISSN 0267-8292 print/ISSN 1366-5855 online © 2002 Taylor & Francis Ltd
http://www.tandf.co.uk/journals
DOI: 10.1080/02678290110096397

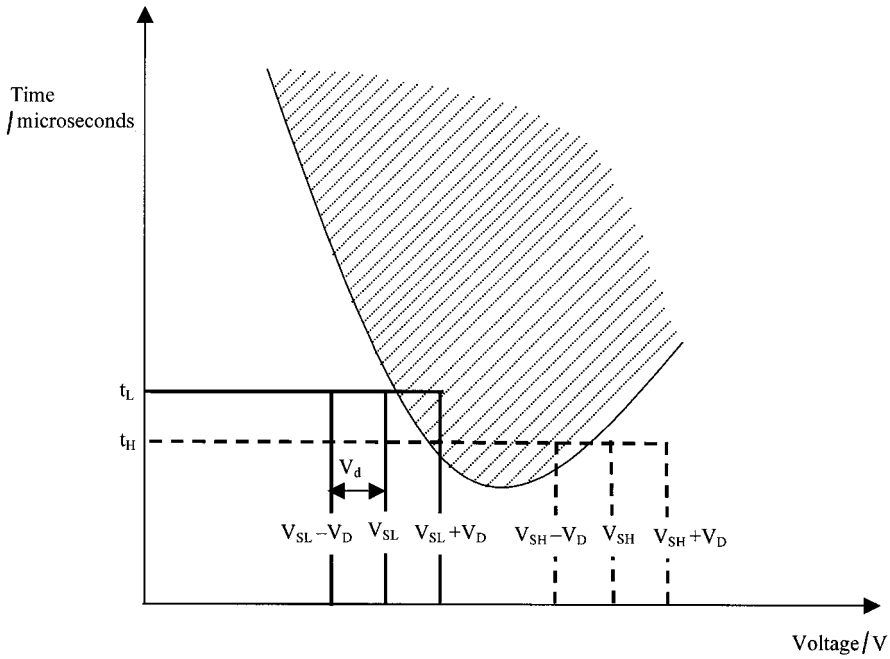

Figure 1. A typical plot of pulse width against voltage, which shows 'anomalous' switching characteristics due to the high biaxiality property of the material. The shaded region gives the value of voltage and pulse width which will produce switched states. The solid lines ($V_{SL}-V_D$, V_{SL}, $V_{SL}+V_D$) represent the voltage levels for the low voltage addressing scheme, whilst the dotted lines ($V_{SH}-V_D$, V_{SH}, $V_{SH}+V_D$) represent the voltage levels for the high voltage addressing scheme.

On the contrary, when these pulses are inverted with respect to each other, their amplitudes add to produce a bipolar switching pulse (V_S+V_D). Therefore, it is possible to switch the pixel into a bright or dark state. Two scans are needed to write a complete picture—one scan for writing bright pixels and another for writing dark ones. The Seiko scheme is therefore a four-slot addressing scheme.

2.2. *The Joers Alvey scheme* [5]

The Joers Alvey scheme operates at a voltage higher than V_{min}. The control window consists of two time slots: during the first slot the row voltage is zero, and during the second it consists of a high voltage monopolar pulse of either positive or negative polarity. The superposition of the selection waveform with the data waveform results in either a switching or non-switching sequence. The switching sequence consists of a pulse of magnitude (V_S-V_D), preceded by a V_D pulse of the same polarity. The non-switching sequence consists of a large pulse of amplitude equal to (V_S+V_D), preceded by a V_D pulse of the opposite polarity, as shown in figure 3. It also is a four-slot scheme as two scans are required to write one image.

The addressing schemes described above have been employed in real display devices. So far, the choice of voltages (V_S and V_D) used and the ratio between these voltages have been obtained through trial and error, without a systematic way of determining voltage values that would give optimum switching conditions. In this paper, we hope to describe the t–V characteristics of these addressing schemes by means of a three variable model [6, 7], in order to be able to identify suitable operating regimes and choose the parameters that would lead to optimum switching conditions.

We anticipate that the t–V curve due to a realistic addressing scheme would differ from the t–V curve due to that of a basic bipolar pulse such as that illustrated in figure 1. For example, a real addressing waveform consists of a switching or non-switching waveform within the control window, which is preceded and followed by a stream of random data pulses. The cumulative rms voltage due to these random data pulses then couple to the dielectric anisotropy of the liquid crystal, and this should effectively shift the basic bipolar t–V curve upwards. Furthermore, the polarity and magnitude of the data pulses directly adjacent to the control window are also crucial in determining the t–V curve for that particular waveform. For example, in the Joers Alvey scheme, a switching pulse of magnitude (V_S-V_D) is preceded by V_D of the same polarity, which decreases the biaxial torque and moves the t–V curve down. Conversely, a non-switching pulse which is of magnitude (V_S+V_D) is preceded by a V_D pulse of the same polarity and should enhance the biaxial torque and move the t–V curve up.

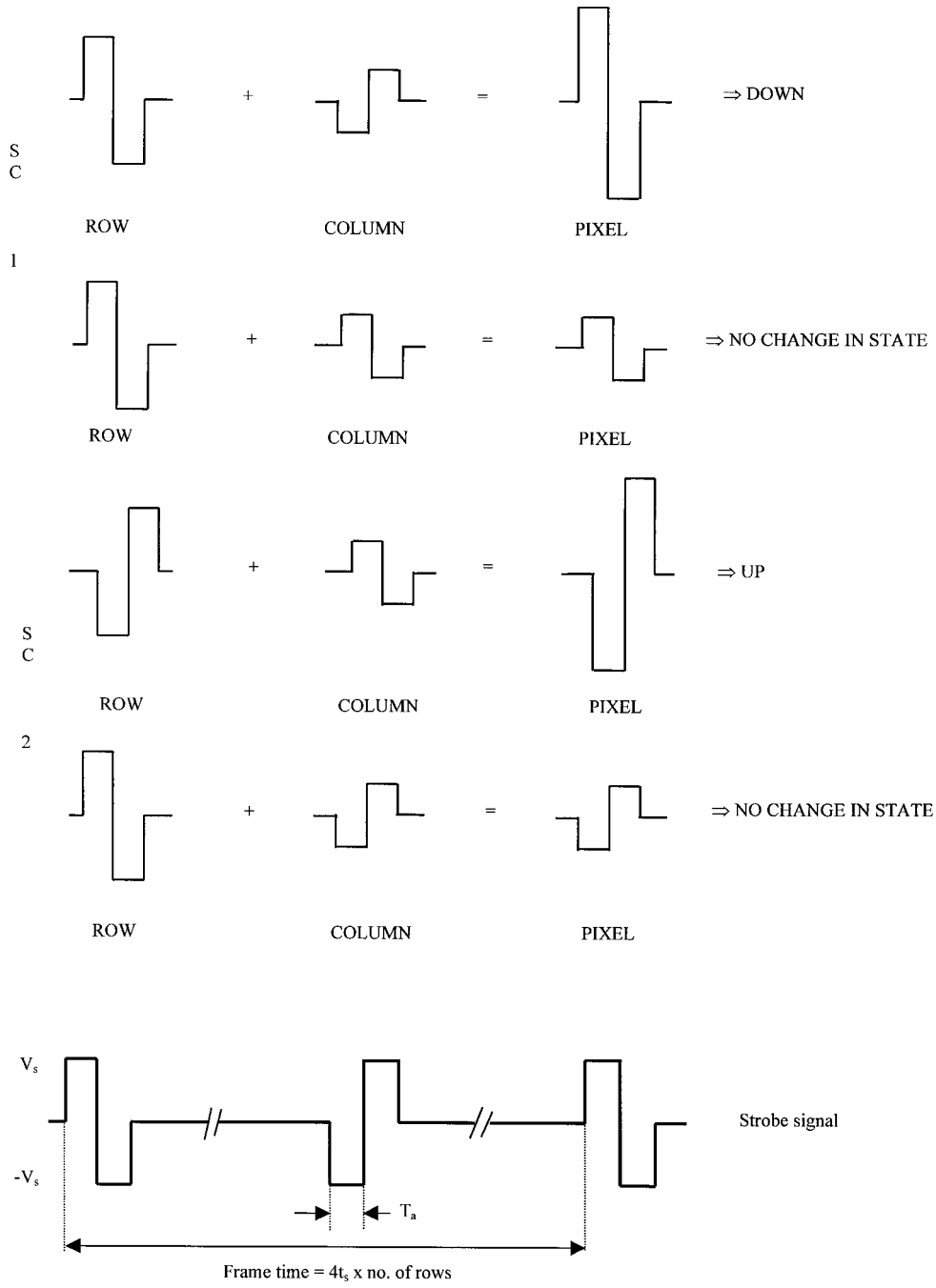

Figure 2. Illustration of the Seiko addressing scheme. During a scan, each row is addressed with a bipolar pulse; the phase of a bipolar column pulse then determines whether the pixel switches to the state selected for the particular scan or if it remains in its current state. This switching scheme is termed a 4-slot scheme corresponding to the 4 pulses (2 × bipolar) applied to each row during a frame.

3. Experimental set-up

The experimental set-up was as follows. A 2 μm thick device filled with SCE8 in a *C*2 stabilized structure was placed between a pair of crossed polarizers. The cell was oriented so that the alignment direction was at 22.5° to the polarizer angle, and kept at an ambient room temperature of 23.0°C. The cell was illuminated with a laser diode, and the optical response of the FLC cell was recorded using a photodiode.

Automated response time measurements were carried out to determine the minimum pulse width (for a given addressing scheme), at a given voltage, required to cause

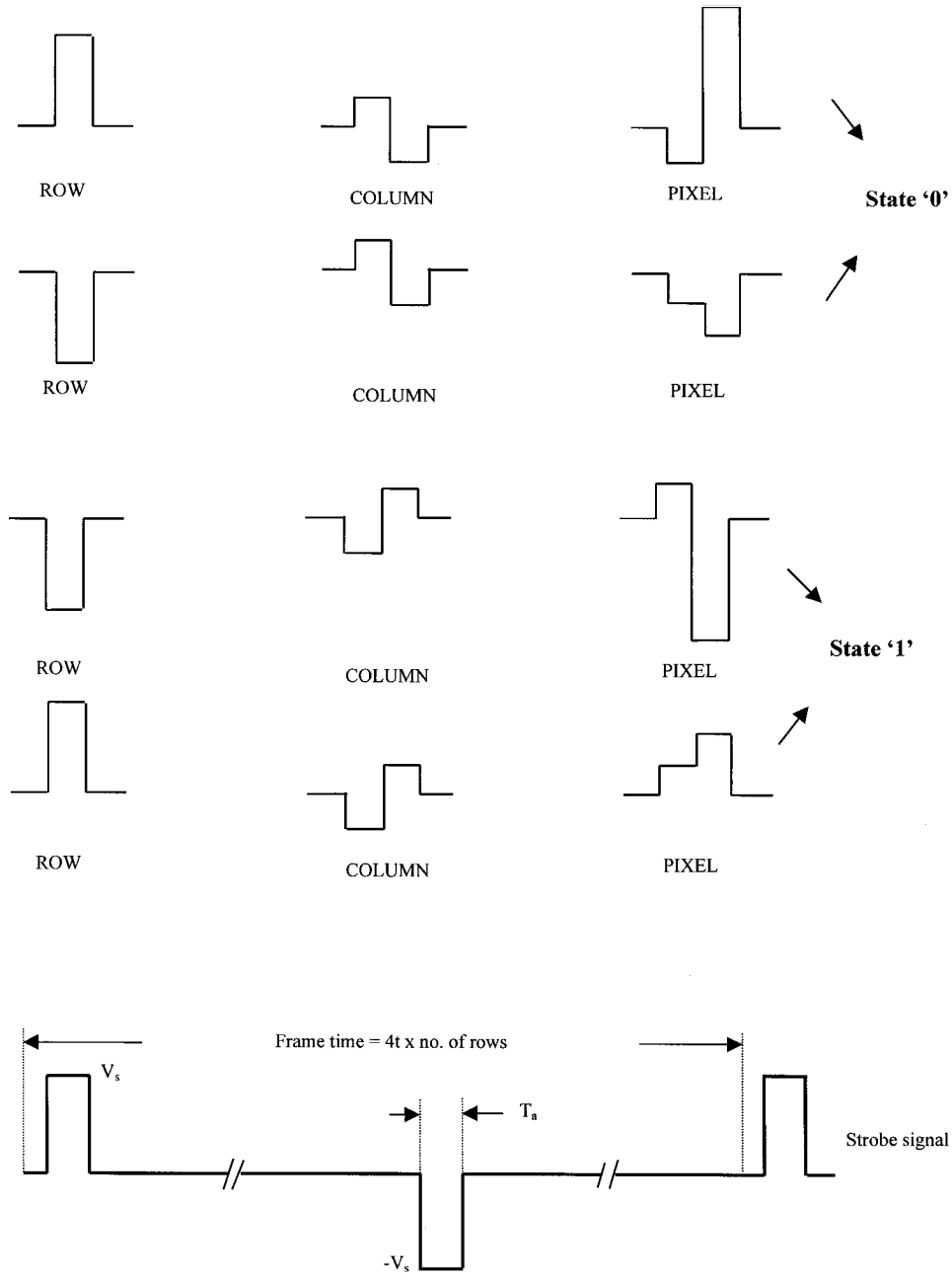

Figure 3. Illustration of the Joers Alvey addressing scheme. During a scan, each row is addressed by monopolar strobe pulses inverted every half frame. The column waveform takes the form of a bipolar pulse. The combination of strobe and data signals gives rise to a non-switching or switching waveform.

latching. A Wavetek 395 arbitrary waveform generator was programmed to output the chosen addressing waveform of a given frequency and amplitude. In order to simulate a real addressing waveform, the switching/non-switching pulses within the control window were preceded and followed by 50 random data pulses. The transmitted intensity extracted by the photodiode was recorded on an oscilloscope, and a schematic illustration of the trace is shown in figure 4. Intensity differences between points (1) and (2) were recorded as a function of pulse width [8], for a range of voltages. Nucleation and growth of domains produce a regime of partial switching between the full and non-switching conditions. With reference to figure 5, the automated measurements were used to determine the 90% and 10% switching points, as the full and non-switching conditions require a subjective judgement. The 10% transmission level is defined as t_{nuc}, the time taken for the nucleation sites to

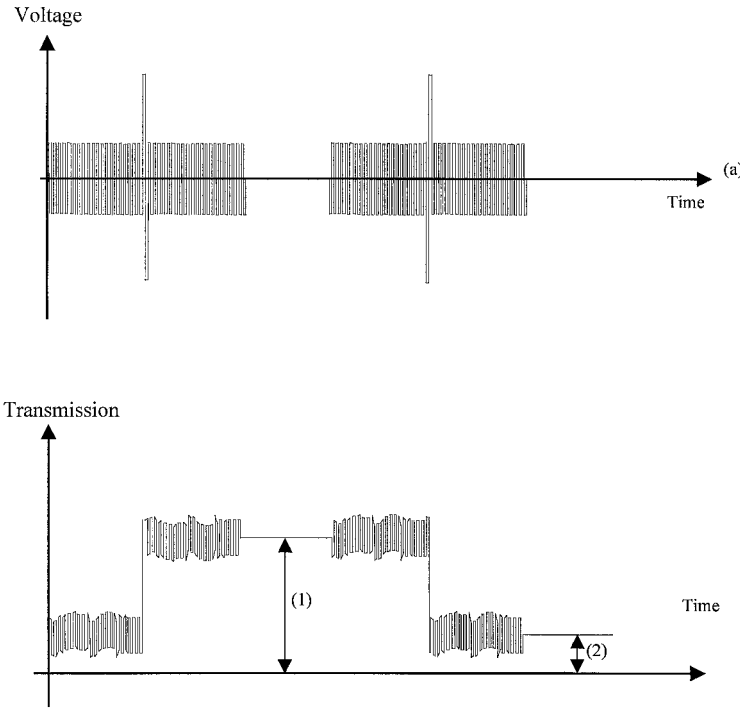

Figure 4. An example of a transmission profile of a cell under the influence of an applied addressing scheme. Transmission levels (1) and (2) are due to switching pulses of opposite polarities.

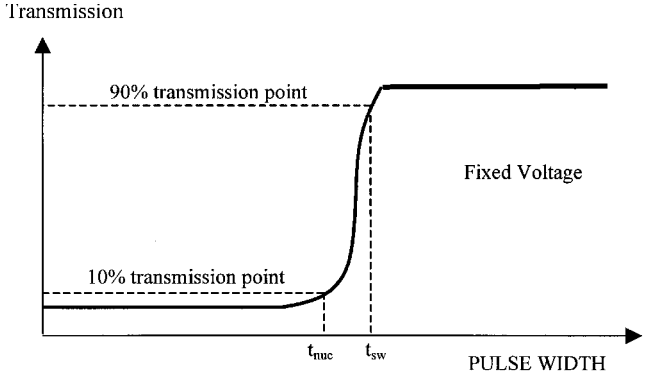

Figure 5. A plot of transmission against pulse width, for a fixed voltage. The 10% transmission level is defined as t_{nuc}, the time taken for the nucleation sites to start to appear; the 90% transmission level is defined as t_{sw}, the time taken for the cell to switch fully to the opposite state.

start to appear, and the 90% transmission level is defined as t_{sw}, the time taken for the cell to switch to the opposite state. We were therefore able to build up a t–V response time curve from the automated data.

3.1. *The effect of random data pulses*

The random data pulses on a pixel resulting from multiplexing should not be able to cause switching under any circumstances, and the random pulses adjacent to the control slot should not affect the switching response. For example, if two random data pulses of equal polarity are adjacent, a pulse of twice the duration is created, and this may lead to spurious switching. Similarly, the random pulses directly adjacent to the control slot can influence the switching significantly. For example a control slot which is meant to switch the device to light may not be able to do this if both the pre- and post-pulse data pulses are of the polarity which switches the device to dark. In order to be sure that a scheme will always work, it is necessary to identify a worst case pulse sequence for the switching and non-switching cases, and investigate these.

The pulse schemes used in this investigation portray the worst case scenario described above, so that we may ensure that a suitable operating regime is found for these addressing schemes. Figure 6 shows the waveforms designed as the worst case scenario for the Seiko scheme. Figure 6 (*a*) has the pre-pulse and the post-pulse both tending to hinder the switching ($V_S + V_D$) pulse, whereas figure 6 (*b*) has the pre-pulse and the post-pulse both tending to induce switching for the non-switching pulse ($V_S - V_D$). Similarly, figure 7 shows the waveforms designed as the worst case scenario for the Joers Alvey scheme. Figure 7 (*a*) has the pre-pulse and the post-pulse both trying to hinder the switching ($V_S - V_D$) pulse, whereas figure 7 (*b*) has the pre-pulse and the post-pulse both tending to induce switching for the non-switching pulse ($V_S + V_D$).

4. Theory

The switching process which takes place in the addressing schemes discussed above involves domain nucleation

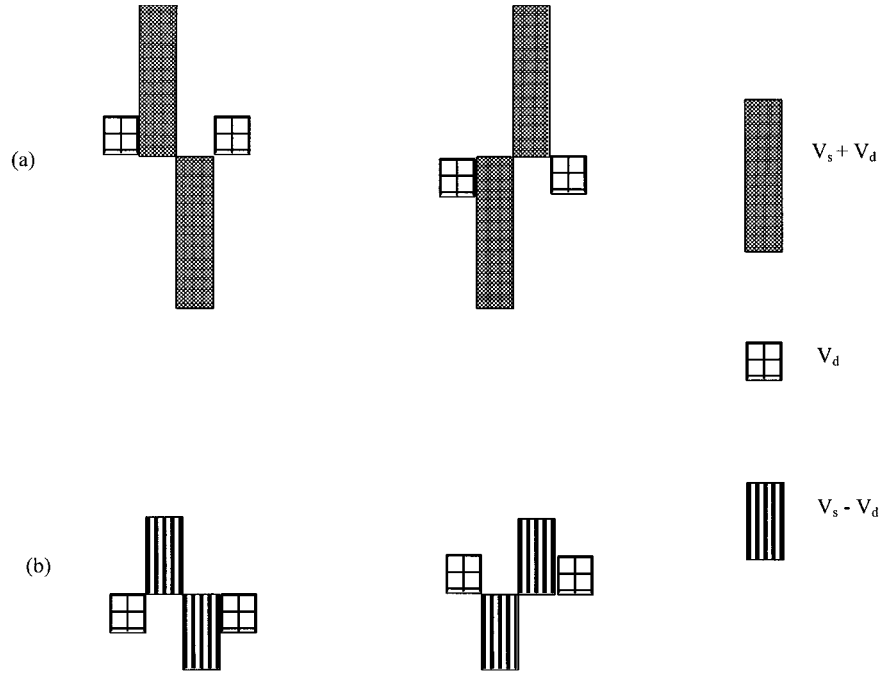

Figure 6. The worst case configurations for the Seiko scheme. (*a*) The switching pulse, (*b*) the non-switching pulse. The ratio $V_s : V_d$ is 4 : 1, giving a switching to non-switching ratio of 5 : 3.

and growth [9]. In a previous paper [10], we described in detail how the switching process may be described by the 'Three Variable Model in One Dimension'. Here we will briefly summarize the model, and use it in analysing the addressing schemes presented above. The three variables are as follows: (i) $\phi_1(z)$ is the director orientation for the background state and is a function of the distance across the thickness of the cell (which we choose to be in the z direction); (ii) $\phi_2(z)$ represents the director orientation within the switched domains through the thickness of the cell; and (iii) A represents the ratio of the domain area to the total device area.

We assume that the cell comprises tilted smectic layers in a chevron configuration [11]. The director reorientation $\phi(z)$ (for the domain or background) will be modelled in each half of the chevron structure using a simple equation of the form:

$$\eta \frac{\partial \phi}{\partial t} = K \frac{\partial^2 \phi}{\partial t^2} + \mathbf{P}_s \mathbf{E} \cos \phi \cos \delta - \partial \varepsilon \varepsilon_0 \mathbf{E}^2 \cos \phi \sin \phi \cos^2 \delta - \varepsilon_0 \mathbf{E}^2 \Delta \varepsilon \cos \phi \times \left[\frac{1}{4} \sin 2\theta \sin 2\delta - \sin \phi \cos^2 \delta \sin^2 \theta \right]$$

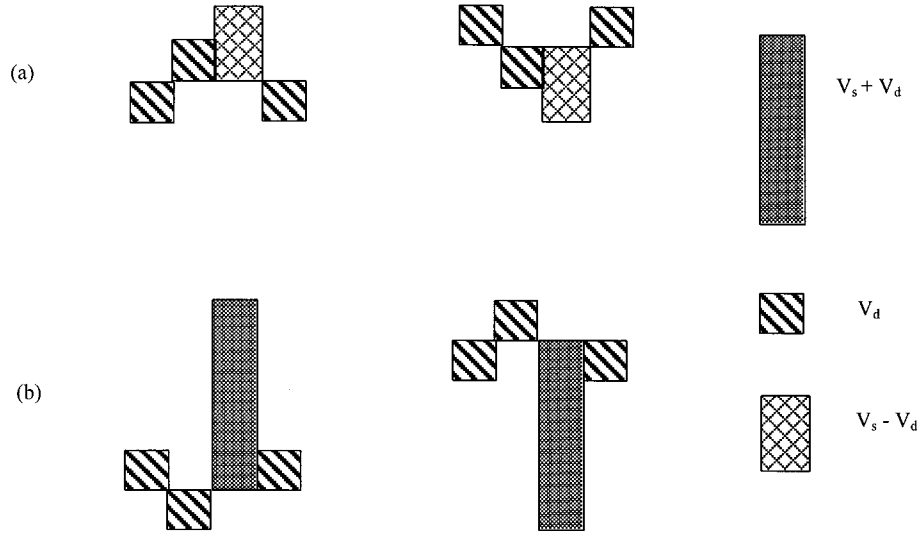

Figure 7. The worst case configurations for the Joers Alvey scheme. (*a*) The switching pulse, (*b*) the non-switching pulse. The ratio $V_s : V_d$ is 3 : 1, giving a switching to non-switching ratio of 2 : 1.

where η_b is the rotational viscosity within the bulk of the SSFLC cell, $\phi(z)$ is the azimuthal angle (background or domain), $\mathbf{P}_s$ is the material's spontaneous polarization, $\mathbf{E}$ is the applied electric field, θ is the cone angle, δ is the chevron tilt angle, K is the elastic constant of the material, $\partial\varepsilon$ is its dielectric biaxiality and $\Delta\varepsilon$ its dielectric anisotropy.

The director within the device is assumed to be fixed at the liquid crystal–glass boundary, with the angle $\phi = 0°$ at the top surface, and $\phi = 180°$ at the bottom surface. The chevron interface is treated as an internal surface, and may be described as

$$T = T_0(2\cos\phi_0 \sin\phi - \sin 2\phi) \quad \text{for the background region}$$

and

$$T = T_{ch}(2\cos\phi_0 \sin\phi - \sin 2\phi) \quad \text{for the domain region,}$$

where T_0 is the chevron interface torque for the background region and T_{ch} is the chevron interface torque for the domain region. T_{ch} is defined to be smaller than T_0 so that when the electric field is applied, the director at the chevron interface is able to switch from $+\phi_0$ to $-\phi_0$ at certain points where the chevron interface torque is weak (i.e. equal to T_{ch}). This leads to nucleation of domains at these points, and the time taken for this to occur is defined as t_{nuc}. These domains then start to grow from these nucleation sites, and the area growth rate [12] as described by Avrami is:

$$\frac{dA}{dt} = Rv\sqrt{N}(1-A)\left[\ln\left(\frac{1}{1-A}\right)\right]^{1/2}$$

where A is the fraction of switched area, N is the number of domains which nucleated at time t_{nuc} and v is the domain wall velocity.

These domains are allowed to grow until A reaches 0.9999, when the cell is defined as having fully switched to the opposite state.

4.1. *Numerical implementation*

The governing equations above were translated into a discrete form, to allow numerical modelling of the switching process. The device was modelled by dividing the FLC into a finite number of thin layers across the thickness of the cell, and computing the value of ϕ within each layer. The value of ϕ at each position was calculated using the forward difference method in the time domain and the central difference method in the space domain. In order to simulate the addressing waveform, the electric field in the model was varied according to the pulses illustrated in figures 6 and 7. In order to simulate realistically an addressing waveform for a display, we have also included in our model 50 random data pulses before and after the control window, as we have similarly done in our experiment. Parameters for the model were then chosen, in order to obtain a good fit to experimental data for the t_{nuc}–V and t_{sw}–V curves of the addressing schemes. The parameters used in this model are shown in the table.

Table. List of parameters used in the Three Variable Model in One Dimension. They are determined by comparisons between data and the predictions of the model.

Parameter	Value
$\mathbf{P}_s$	6.3 nC cm^{-2}
K	6.5×10^{-12} N
θ	19.02°
δ	17.02°
$\partial\varepsilon$	0.52
$\Delta\varepsilon$	−1.92
η	0.079 N sm^{-2}
T_0	0.055 N m^{-1}
T_{ch}	1.485×10^{-3} N m^{-1}
d	2.0 μm

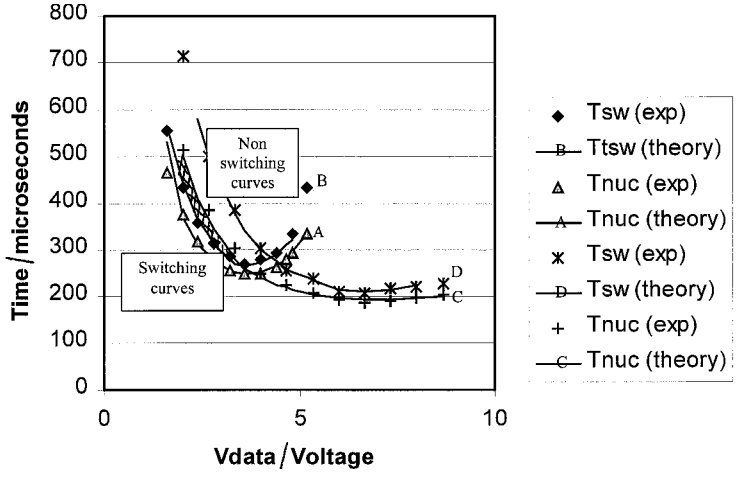

Figure 8. The experimental results and theoretical fits of the t–V curve for the worst case configuration of the Seiko addressing scheme. The operating regime is the narrow shaded region between curves B and C.

The resulting director profile may also be used to obtain the transmission through the cell, using the Berreman 4×4 matrix programme. The transmission from the model may then be compared with the transmission obtained from experiment, in order to confirm whether the parameters that we have chosen in the model are indeed appropriate. For example, the relaxation rate of the transmission is a good measure of the elastic torque acting on the directors.

5. Comparison of results from experiment and theory

The data points in figure 8 show the experimental results of the t–V plots for the worst case scenario of the Seiko addressing scheme, where the continuous lines are the theoretical predictions. Curves A and B show the t–V curves for worst case switching: the region below curve A indicates the non-switching regime, the region above curve B indicates the switching regime, and the region between these two curves is the partial switching regime. Correspondingly, curves C and D show the t–V curves for worst case non-switching: the region below curve C indicates the non-switching regime, the region above curve D indicates the switching regime, and the region between the two curves is the partial switching regime. Therefore, the useful operating region (i.e. switching occurs when it is supposed to, and likewise for the non-switching case) lies between curves B and C. The region of operation between curves B and C is actually quite narrow due to the need to switch the device fully with the switching pulse and avoid any domain nucleation for the non-switching pulse. The 'Three Variable Model in One Dimension' correctly reproduces this narrow operation regime, which would not be correctly reproduced using a model which did not allow for domain nucleation and growth. This model also accurately replicates the shape of the experimental t–V curve, i.e. the worst case switching curve contains a pre-pulse that is of the same polarity as the leading bipolar pulse, and this serves to enhance the biaxial torque and shifts the 'switching' t–V curve up in comparison to the 'non-switching' t–V curve.

As noted above, the continuous lines in figure 8 indicate the theoretical predictions for each of the curves described, and they show an excellent fit to the experimental data. In figure 9, we compare the transmission as a function of time produced by experiment and theory; these look remarkably similar. The correct modelling of this transmission curve again relies on the fact that the model correctly reproduces the effect of domain nucleation and growth.

We can also note that the relaxation profile at point (i), figure 9 (*a*), for the experimental plot is successfully duplicated in theory by choosing an appropriate elastic constant. The elastic constant (6.5×10^{-12} N) provided

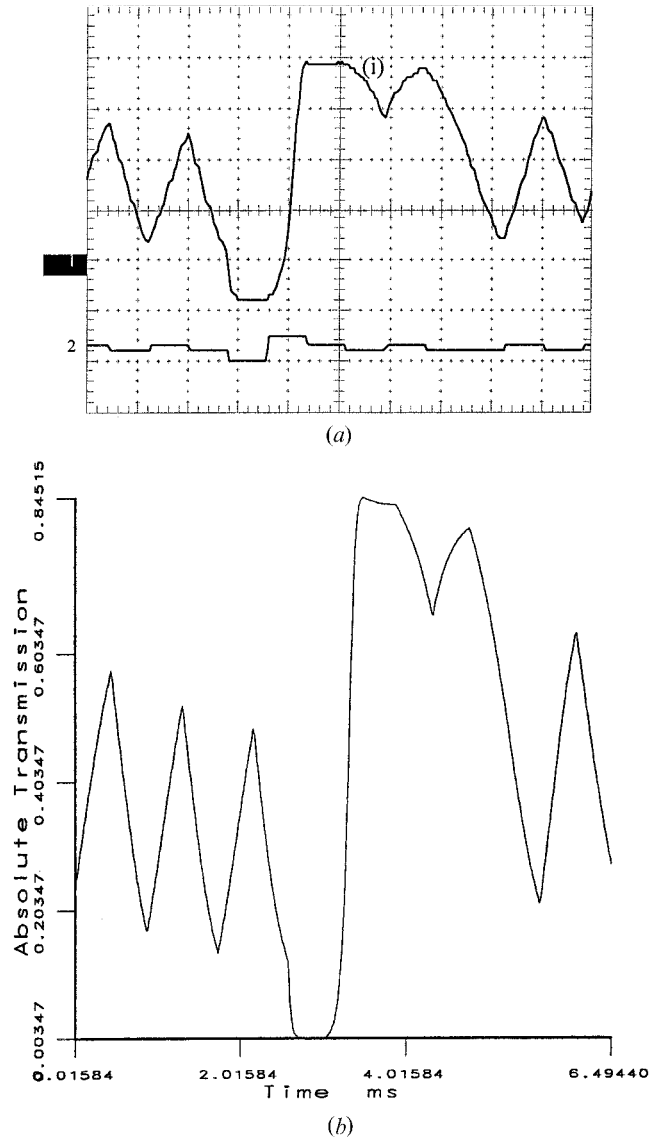

Figure 9. The transmission profile obtained in (*a*) experiment, and (*b*) theory, for the Seiko addressing scheme. A correct value of the elastic constant within the model is essential in order to duplicate the experimental transmission profile. For example, an elastic constant of 6.5×10^{-12} N was required so that the relaxation profile at point (i) would be identical for the experimental and theoretical plots.

a theoretical relaxation profile which was similar to that produced by the experiment. It should be noted that the values of the elastic constant and other parameters which were found to give a good fit to the experimental data, are very similar to the parameter values measured by other workers [13, 8].

6. Prediction of results for the Joers Alvey scheme

In order to test the 'Three Variable Model in One Dimension' further, we have taken the parameters used in the fitting of the Seiko scheme and used the model

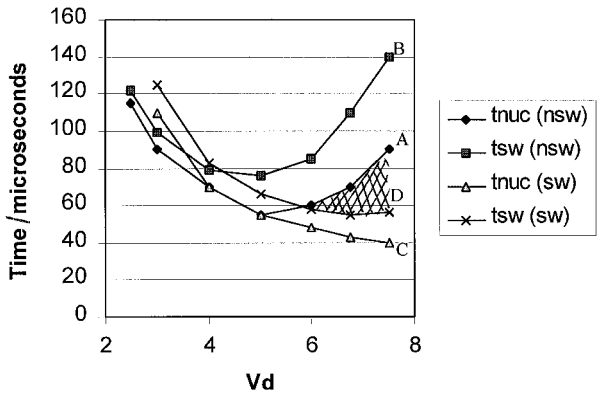

Figure 10. The theoretical t–V curve for the worst case configuration of the Joers Alvey addressing scheme. The operating regime is the shaded region between curves A and D.

to predict the operating region for the Joers Alvey addressing scheme. With reference to the parameters listed in the table, and the pulse sequences illustrated in figure 3 using a $V_S : V_D$ ratio of 3 : 1, we plot in figure 10 the theoretical switching and non-switching curves for the Joers Alvey scheme. The resulting plot is a realistic representation of what we would expect of a t–V curve due to a Joers Alvey scheme. With reference to figure 7, we note that the switching waveform consists of two pulses of the same polarity, for example $+V_D$ followed by $+(V_S - V_D)$ and the resultant t–V curve is shifted down and has a 'flatter' minimum compared with the non-switching curve due to the decrease in dielectric torque. On the other hand, the non-switching waveform consists of two pulses of opposite polarity, for example $+V_D$ followed by $+(V_S + V_D)$, which serves to enhance the dielectric torque and shifts the t–V curve upwards.

With reference to figure 10, we notice that the pulse width taken to switch using this scheme is much shorter than the pulse width taken to switch due to a Seiko scheme; i.e. a range of 45–60 μs for the Joers Alvey scheme, compared with a range of 250–500 μs for the Seiko scheme. The range of pulse widths predicted using our theory for the Joers Alvey scheme is also comparable to the pulse widths employed in practical Joers Alvey addressing schemes [14]. These results reflect the success of the high voltage Joers Alvey scheme in reducing the pulse widths required for switching, compared with the much slower low voltage Seiko scheme.

Again it is important to note the strength of the prediction from the 'Three Variable Model in One Dimension' for both the Seiko and Joers Alvey schemes: the width of the switching regime is predicted accurately as it allows for domain nucleation and growth, and its consequent partial switching effect.

7. Conclusion

In this paper we have experimentally determined the operating regime for the Seiko addressing scheme, and taken into consideration the worst case configuration due to random data pulses. We then showed that our 'Three Variable Model in One Dimension' is a simple but powerful model that is able to duplicate the t–V characteristics of these addressing schemes under a wide range of operating voltages. We have also used this model to predict the operating regime for the high voltage Joers Alvey scheme. Our model is also able to reproduce accurately the transmission obtained experimentally, hence confirming that our 'Three Variable Model in One Dimension' is able to simulate realistically the switching process due to complicated addressing schemes. In future modelling of addressing schemes, we propose to include ionic effects. This effect will be especially useful in modelling addressing schemes which contain blanking pulses, for example, which induce ionic polarization within the device.

References

[1] Maltese, P., Piccolo, R., and Ferrara, V., 1993, *Liq. Cryst.*, **15,** 819.
[2] Hughes, J. R., and Raynes, E. P., 1993, *Liq. Cryst.*, **13,** 597, errata corrige **15,** 281.
[3] Yeoh, C. T. H., Lister, S. J. H., Mosley, A., and Nicholas, B. M., 1992, *Ferroelectrics*, **132,** 293.
[4] Matuszczyk, T., and Maltese, P., 1995, *Proc. SPIE*, **2372,** 296.
[5] Surguy, P. W. H., Ayliffe, P., Birch, M. J., Bone, M. F., Coulson, I., Crossland, W. A., Hughes, J. R., Ross, P. W., Saunders, F. C., and Towler, M. J., 1991, *Ferroelectrics*, **122,** 63.
[6] Ulrich, D. C., and Elston, S. J., 1995, *J. appl. Phys.*, **78,** 4331.
[7] Pabla, D. S., and Elston, S. J., 1997, *Liq. Cryst.*, **22,** 525.
[8] Dunn, P., 1998, PhD thesis, University of Exeter, UK.
[9] Handschy, M. A., and Clark, N. A., 1982, *Appl. Phys. Lett.*, **41,** 1.
[10] Said, S. M., and Elston, S. J., 2001, *Liq. Cryst.*, **28,** 561.
[11] Rieker, T. P., Clark, N. A., Smith, G. S., Parmar, D. S., Sirota, E. B., and Safinya, C. R., 1987, *Phys. Rev. Lett.*, **59,** 2658.
[12] Ishibashi, Y., 1995, *Jap. J. appl. Phys.*, **24,** *suppl.* **242,** 126.
[13] Brown, C. V., and Jones, J. C., 1999, *J. appl. Phys.*, **86,** 1.
[14] Matuszczyk, T., 1995, PhD thesis, Chalmers University of Technology, Göteborg, Sweden.